Yoshikay-Benitez *et al.*
Journal of Wood Science (2023) 69:12
https://doi.org/10.1186/s10086-023-02086-1

Journal of Wood Science

ORIGINAL ARTICLE

The *Populus alba* cationic cell-wall-bound peroxidase (CWPO-C) regulates plant growth, lignin content and composition in poplar

Diego Alonso Yoshikay-Benitez[1], Kaori Ohira[1], Kasturi Banerjee[1], Koki Fujita[2], Jun Shigeto[2,3*] and Yuji Tsutsumi[2*]

Abstract

Cationic cell-wall-bound peroxidase (CWPO-C) from *Populus alba* is the only Class III peroxidase that has been shown to be able to oxidize high molecular weight lignin polymers from sinapyl alcohol and previously, has been believed to be a lignin polymerization-specific peroxidase. However, using an Arabidopsis heterologous expression system, we showed recently that CWPO-C contributes to differentiation or early growth and is involved in auxin catabolism. In this study, to clarify the function of CWPO-C in poplar, we analyzed *CWPO-C* gene expression and phenotypic changes with *CWPO-C* overexpression and suppression. Real-time PCR and monitoring promoter activity of *CWPO-C* using β-glucuronidase (GUS) assay revealed that *CWPO-C* was strongly expressed in immature tissues, such as the upper stem, axillary buds, and young leaves, in addition to expression in developing xylem. In transgenic poplars in which the expression of *CWPO-C* was upregulated or suppressed, changes in stem growth, gravitropism bending time, lignin content and syringyl/guaiacyl (S/G) composition were observed. Overexpressing *CWPO-C* enhanced stem growth and gravitropic response (shorter bending time). With suppressed *CWPO-C* expression, the lignin content was reduced approximately 45% and the S/G ratio decreased by half. These results strongly suggest that CWPO-C plays a role in differentiation and early growth, as well as in lignin polymerization.

Keywords *Populus alba*, CWPO-C, Plant peroxidase, Overexpression, Suppression, Plant growth, Gravitropism, Lignin, S/G ratio

Introduction

Class III plant peroxidases are encoded by a large gene family, and poplar (*Populus trichocarpa*) contains 93 genes [1]. The peroxidases differ in their individual substrate oxidation activities and physiological roles [2]. While the roles of peroxidases in various processes, such as lignification [2, 3], plant defense [4], development [5, 6], germination [6–8], and seed longevity [9] have been reported, to date, relatively few peroxidases have been functionally annotated, and the in vivo function of most peroxidases remains unclear. In lignin biosynthesis, peroxidases use hydrogen peroxide in oxidizing monolignols (coniferyl and sinapyl alcohols in angiosperms), and the resulting radicals (G, guaiacyl and S, syringyl units) are polymerized into lignin [10]. Lignin polymerization also

*Correspondence:
Jun Shigeto
jshigeto@hiroshima-u.ac.jp
Yuji Tsutsumi
y-tsutsu@agr.kyushu-u.ac.jp
[1] Department of Agro-Environmental Sciences, Graduate School of Agriculture, Kyushu University, 744 Motooka Nishi-Ku, Fukuoka 819-0395, Japan
[2] Faculty of Agriculture, Kyushu University, 744 Motooka Nishi-Ku, Fukuoka 819-0395, Japan
[3] Headquarters for Research in Collaborative Sciences Enabling the Future, Hiroshima University, 1-3-2 Kagamiyama, Higashihiroshima 739-8511, Japan

requires the oxidization of the phenolic groups in lignin to continue the polymer growth [11]. So far, only CWPO-C peroxidase has been demonstrated to have oxidation activity toward large-size phenolic substrates, such as S-oligo (polymerized oligomeric sinapyl alcohol) [12, 13]. The oxidation of phenolic substrates occurs at the amino acid residues, Tyr74 and Tyr177, avoiding steric hindrance of the substrates and proximity with the heme pocket [14, 15]. This oxidation capability makes CWPO-C a unique peroxidase, and because of its unique oxidizing abilities, previously CWPO-C has been believed to be a lignin polymerization-specific peroxidase.

Previously, *CWPO-C* promoter analysis in Arabidopsis using β-glucuronidase (*GUS)* as a reporter gene revealed that it was strongly expressed in immature tissues, regardless of the organ [16]. We also reported that transgenic Arabidopsis plants overexpressing *CWPO-C* exhibited suppression of stem elongation and seed development with an unexpected phenotype: stem tip curled in overexpressing plants was about 60% of that in the wild type [16]. These results, using a heterologous *CWPO-C* expression system, suggested that *CWPO-C* is involved in plant organ development or early growth. Other reports using heterologous peroxidase expression suggested that peroxidases are involved in plant development and growth. Overexpression of peroxidase *CpPrx01* in *Arabidopsis thaliana* enhanced stem growth [5]. Overexpressed *HRP-C1a* in *Nicotiana tabacum* and hybrid poplar resulted in faster growth and longer stems [17, 18]. Plant growth and organ development are regulated via extremely complex networks involving molecules, such as phytohormones.

Heterologous expression using Arabidopsis has the advantage that it can be analyzed throughout one generation in approximately 3 months; however, there are some cases, where its expression pattern differs from poplar, which might be because of differences in the properties of the transcription regulating factors, and so on. A further limitation is that a reverse genetic strategy for the suppression of the targeting *CWPO-C* gene is not available in the heterologous expression system. In this study, we prepared and analyzed transgenic poplar plants to confirm the expression pattern of *CWPO-C* and to investigate the role of CWPO-C in poplar development, growth and lignification using overexpression and suppression of *CWPO-C*.

Materials and methods

Generation of transgenic plants

Preparation and construction of plasmids for GUS assays and *CWPO-C*-overexpression were as described by Yoshikay-Benitez et al. [16]. Both, the CWPO-C overexpression and suppression (RNAi) constructs were driven by the Cauliflower Mosaic Virus 35S promoter (CaMV 35S). For construction of the RNAi silencing vector, a hairpin-type gene cassette including a 432-bp fragment of *CWPO-C* open reading frame from nucleotides 633 to 1064 (relative to the ATG start codon) was connected between *Bam*HI and *Sac*I sites of pBF2.

Transformation of poplar was performed as described by Takata and Eriksson [19], Song et al. [20] and Nanasato et al. [21] with some modifications. Briefly, stems from wild-type *Populus alba* were excised (1 cm length), and *Agrobacterium tumefaciens* strain LBA4404 carrying the binary vector as above was used to transfect explants. Explants were transfected in Murashige–Skoog (MS) medium, pH 5.6, 1× MS vitamins, 3% (*w*/*v*) sucrose, *A. tumefaciens* at $OD_{600}=0.4–0.9$, 20 μM acetosyringone and 0.015% Silwet L-77 for 1 h with shaking at 60 rpm. Co-cultivation of explants was performed in the dark for 3 days in MS medium, pH 5.6, 0.3% Gelrite and three layers of filter paper No. 2 pre-wetted with 5 μM acetosyringone in liquid MS medium. After co-cultivation, the explants were washed twice with sterile water and once with MS medium, pH 5.6, with 1× MS vitamins, 3% sucrose and 50 mg/L meropenem. Finally, explants were blotted on filter paper and transferred to MS medium, pH 5.6, 1× MS vitamins, 3% (*w*/*v*) sucrose, 0.3% Gelrite, 0.2 mg/L 6-benzyl amino purine (BAP), 0.1 mg/L indole-3-butyric acid (IBA), 0.01 mg/L thidiazuron (TDZ), 50 mg/L kanamycin and 50 mg/L meropenem. The culture medium was renewed every 3 weeks. Callus formation was observed after 3–6 weeks. For induction of multiple shoots, callus was transferred onto 0.3% Gelrite-solidified MS medium, pH 5.6, with 1× MS vitamins, 3% (*w*/*v*) sucrose, 0.2 mg/L BAP and 0.01 mg/L TDZ, and was cultured in a growth chamber (CLE-303; TOMY SEIKO Co., Ltd., Tokyo, Japan) at 25 ± 1 ℃ under 16 h light (65 μmol photons m^{-2} s^{-1} from cool-white fluorescent tubes) and 8 h dark.

Plant materials and growth conditions

Populus alba wild type and transgenic plants were cultured on 0.3% Gelrite-solidified MS medium, pH 5.6, with 1× MS vitamins and 3% (*w*/*v*) sucrose, 50 mg/L kanamycin (only for transgenic plants) in plant boxes. They were incubated in the growth chamber, as above.

Preparation of stem cryosections

For cryostat sectioning, stem pieces 5 mm in length were vacuum-incubated with 30% sucrose for 10 min, immersed in the mixture of Cryomatrix (Thermo scientific, USA) and 30% sucrose (1:1) for 10 min, then incubated in Cryomatrix for 10 min. Finally, Cryomatrix-embedded sections were mounted in a plastic cryomold (Tissue-Tek, The Netherlands), snap-frozen in liquid

nitrogen, and stored at − 80 °C. Sections of the stem were cut with a cryostat (Thermo Scientific HM 525 Cryostat, VWR International, PA, USA) at − 15 °C, and mounted on glass slides for histochemical staining or on PEN-membrane 2.0 µm glass slides (Leica, Germany) for RNA extraction. Prior to laser micro-dissection, the 25 µm sections were fixed in cold RNase-free 99.5% ethanol at − 20 °C for 10 s, washed of Cryomatrix compound with RNase-free water for 2 min, and refixed in cold RNase-free 99.5% ethanol at − 20 °C for 1 min. All instruments and reagents were treated to make RNase-free to avoid RNA degradation.

Laser micro-dissection of stem cryosections

Sections mounted on PEN glass slides were air-dried and micro-dissected with a laser micro-dissection (LMD) microscope (LMD7, Leica Microsystems CMS GmbH, Wetzlar, Germany) at room temperature. The LMD technique was combined with RNA isolation and transcript analysis by real-time quantitative PCR (RT-qPCR). LMD was performed as described by Abbott et al. [22] with adaptations for the cell and tissue types used. For optimal dissection we used the maximum laser intensity and the slowest cutting speed. Different micro-dissected tissues were collected individually into the cap of nuclease-free 0.5 mL PCR tubes (Axygen, Union City, CA, USA) containing 60 µL lysis buffer supplied with the RNAqueous-Micro RNA Kit (Ambion, Inc., Austin, TX, USA). The collected dissection samples were kept in liquid nitrogen until they were subjected to RNA extraction.

RNA extraction and real-time PCR

Total RNA from micro-dissected tissues was isolated using the RNAqueous-Micro-RNA Kit (Ambion, Inc., Austin, TX, USA). The RNA was treated with DNase I inactivation reagent supplied with the kit. First-strand cDNA was synthesized using ReverTra Ace® (Toyobo Co., Japan). The cDNA solution was used as template for PCR. The primer sequences for the *CWPO-C* gene were: *CWPO-C*-left (GCTCGTGATTCTGTTGTTTTGACA AAG), *CWPO-C*-right (GCTGCAAACTTCTGTTTC TGCAC) and for the reference gene *UBQ* (BU879229): *UBQ*-left (TTCACTTGGTGCTGCGTCTC), *UBQ*-right (TCTGAGCTCTCGACCTCCAG). The copy numbers of the fragments for each target gene were estimated as described by Takeuchi et al. [23] with adaptations for the tissue types used. The relative quantity of the target mRNA was normalized using *UBQ* gene as an internal standard.

Western blot analysis

Western blot was done as described by Yoshikay-Benitez et al. [16] using an anti-CWPO-C antibody and the anti-rabbit IgG secondary antibody conjugated with horseradish peroxidase (Proteintech Group Inc., Japan) at a dilution of 1:250 (*v*/*v*) and 1:500 (*v*/*v*) in 1× PBS (pH 7.4), respectively. Briefly, a 15 µg protein sample was separated by 10% (*w*/*v*) SDS–polyacrylamide gel electrophoresis and then electroblotted onto a PVDF membrane (Merck Millipore Ltd., Tullagreen, Ireland). PVDF membranes were blocked overnight using 5% (*w*/*v*) skimmed milk dissolved in 1× PBS buffer. Membranes were blotted with the antibody then washed twice in 1× PBS and probed with a goat anti-rabbit IgG horseradish peroxidase conjugate (Proteintech Group Inc., Japan). After washing the membrane twice in 1× PBS, the immunopositive bands were visualized using WSE-7140 EzWestBlue W (ATTO). Other 15 µg protein samples were separated by electrophoresis and stained with Coomassie Brilliant Blue (CBB) to detect Rubisco.

GUS staining

GUS staining of transgenic poplar bearing *Pcwpo-c*::*GUS* was done as described by Vitha et al. [24]. Briefly, transgenic poplar organs were incubated with 0.5% paraformaldehyde for 45 min at − 0.07 MPa vacuum to infiltrate the fixation agent. Then, after washing twice in 100 mM phosphate buffer (pH 7), the samples were transferred to GUS staining solution containing 100 mM $NaPO_4$, 0.5 mg/mL x-gluc (5-bromo-4-chloro-3-indolyl-β-D-glucuronide), 0.2 mM $K_3Fe(CN)_6$, 0.2 mM $K_4Fe(CN)_6$, pH 7, and incubated overnight. Subsequently, samples were post-fixed in 60% ethanol, 5% acetic acid, 3.7% formaldehyde solution for 2 h. Finally, samples were dehydrated with an ethanol concentration gradient (70%, 80%, 90%, 100%) for 1 h each and chloral hydrate/water/glycerol (25:9:3, *w*/*w*) solution overnight to clear the tissues.

Determination of acetyl bromide-soluble lignin (ABSL)

Stem samples were harvested from 6-week-old wild-type plants and each transgenic line. They were ground to a powder in liquid nitrogen and then extracted with three washes of methanol. The extractive-free sample was freeze dried (CS-110 Scanvac, Lynge, Denmark) and used for further lignin analysis. The acetyl bromide lignin assay was performed as described by Barnes and Anderson [25]. The extractive-free, freeze-dried sample (ca. 5 mg) was digested with 1 mL of 25% acetyl bromide at 70 °C for 1 h in a glass vial, immediately cooled in ice, then 5 mL glacial acetic acid was added to complete the reaction. Later, 450 µL of the diluted sample was mixed with 1200 µL of 1.5 N NaOH and 900 µL of 0.5 M hydroxylamine hydrochloride, and the volume was adjusted to 3 mL with acetic acid. The absorbance at 280 nm of the mixture was recorded using a spectrophotometer (Shimadzu UV-1850, Japan). A blank sample

was run as a control. The content percentage of lignin = $100 \cdot V \cdot (A_{sample} - A_{blank}) / \varepsilon \cdot D \cdot L$ [where V = volume of the final solution (L); A = absorbance; ε = molar extinction coefficient ($g^{-1} \cdot L \cdot cm^{-1}$); D = dry weight of the sample (g); L = cell thickness (cm)]. A molar extinction coefficient of 22.5 $g^{-1} \cdot L \cdot cm^{-1}$ was used for the calculation of percentage ABSL content.

Derivatization followed by reductive cleavage (DFRC)

The DFRC method was performed as described by Lu and Ralph [26]. Briefly, 10 mg of extractive-free sample in 3 mL acetyl bromide reagent (acetyl bromide/acetic acid, 20:80, *v*/*v*) was shaken at 90 rpm at 50 °C for 3 h. The solvent was removed by rotary evaporation below 50 °C. The evaporation residue was resuspended in 3 mL acidic reduction solvent (dioxane/acetic acid/water, 5:4:1, *v*/*v*/*v*). Following the addition of 50 mg zinc dust, the mixture was transferred into a separating funnel with 10 mL dichloromethane and saturated ammonium chloride. The internal standard, 0.1 mg of tetracosane, was added, and the aqueous phase was adjusted to between pH 2 and 3 using 3% HCl. After vigorous mixing, the organic layer was collected, and the extraction was repeated twice with 5 mL dichloromethane. The organic layer was dehydrated in magnesium sulfate, redissolved in 1.5 mL dichloromethane, and acetylated overnight with 0.2 mL acetic anhydride and 0.2 mL pyridine. Once acetylation reagents were removed, the samples were dissolved in dichloromethane and subjected to gas chromatography with a flame ionization detector (GC–FID). GC–FID analysis was performed using a Shimadzu GC-2014 (Shimadzu Co., Ltd., Kyoto, Japan) equipped with a InertCap column (0.25 mm × 30 m; GL Sciences Inc., Tokyo, Japan). The temperature was programmed at a rate of 3 °C min^{-1} from 140 to 240 °C and at 30 °C min^{-1} from 240 to 310 °C. The final temperature (310 °C) was held for 12 min. The amounts of coniferyl alcohol and sinapyl alcohol were determined using calibration curves derived from acetylated pure standards.

Histochemical assay and imaging

Cell walls were stained in stem sections of wild type (WT) and transgenic plants using toluidine blue; lignins were detected using Wiesner staining. Plants were collected at 6 weeks, and 20 µm cross sections were cut from the first 0.5 cm of the basal parts of stems. Stems were embedded in Cryomatrix compound, then sections were prepared at − 20 °C. Cryomatrix was removed from the sections with water. Sections were then stained with 0.02% toluidine blue for 5 min [27]. Wiesner staining was performed as described by Euring et al. [28], soaking sections in 1% (*w*/*v*) phloroglucinol for 3 min. Mounted sections were examined with a Keyence VHX-6000 optical microscope.

A time lapse camera TLC200 (Brinno, Taiwan) was used for gravitropic experiments. Poplar plants at 6 weeks were positioned horizontally and imaged every minute for 24 h. The time the stem took to recover the 90° vertical position was recorded.

Results

CWPO-C is expressed in meristematic and developing tissues

Transgenic poplar with the construct expressing the *GUS* gene under the control of the *CWPO-C* promoter (*Pcwpo-c*::*GUS*) was analyzed. GUS assays showed that *Pcwpo-c*::*GUS* transgene was expressed in stem, leaves and roots (Fig. 1a). The upper and middle stem had potent GUS activity (Fig. 1a). The whole of young leaves at the upper stem were GUS stained, and the staining in the leaves tended to fade when the leaf turned older (Fig. 1a). Arabidopsis bearing *Pcwpo-c*::*GUS* also showed strong expression in young leaves [16]. Interestingly, *Pcwpo-c*::*GUS* was expressed in shoot tips (Fig. 1b1) and the base of axillary buds (Fig. 1c1), although our previous studies suggested that CWPO-C protein expression was related to lignin polymerization. Microscopic observation revealed that *CWPO-C* was preferentially expressed in meristematic tissues, the shoot apex and axillary meristems (Fig. 1b2, c2). In addition, Fig. 1d1, 2 shows GUS staining in the developing xylem of the middle stem. To complement the visual expression patterns of *Pcwpo-c*::*GUS*, we applied RT-qPCR analysis to plant organs, where GUS activity was observed: we found *CWPO-C* was more highly expressed in the middle stem than in the shoot tip and other stem parts (Fig. 2).

The *CWPO-C* promoter was preferentially expressed in the shoot tip (Fig. 1b1, 2). The transcript abundance of *CWPO-C* in the shoot tip was further examined by RT-qPCR analysis combined with LMD. As shown in Fig. 3, *CWPO-C* was strongly expressed in the shoot apex (Fig. 3d). In contrast, *CWPO-C* showed lower expression in the stem cambium (Fig. 3d). Results showing high *CWPO-C* expression as determined by RT-qPCR were consistent with the GUS staining observations (Fig. 3b, c). The meristems are responsible for the growth and development of tissues, and the specific expression of *CWPO-C* in meristematic tissues, such as shoot apex and axillary meristems, indicates that CWPO-C might exert a substantive biological function in plant growth and development.

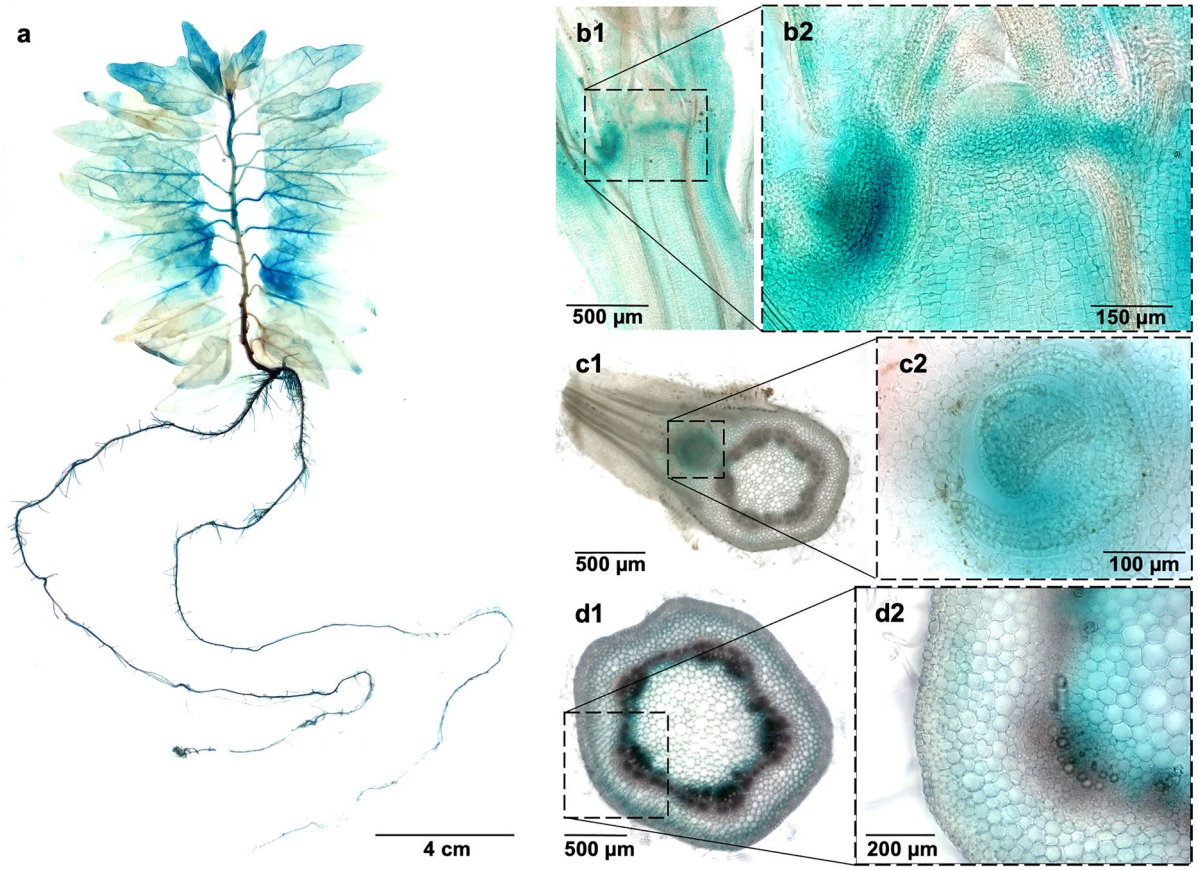

Fig. 1 *CWPO-C* promoter analyses in poplar using *GUS* reporter gene. **a** Whole 6-week-old plant. **b1** Longitudinal section of shoot tip, **b2** Longitudinal section of shoot apex. **c1** Cross section of axillary bud, **c2** Cross section of axillary meristem. **d1** and **d2** Cross section of developing xylem in the middle stem

Considering these results, and also our previous report using heterologous expression system in Arabidopsis showing that *CWPO-C* promoter activity was observed in any immature organs including leaf, stem, root, flower and fruit, it can be assumed that CWPO-C is involved in development or differentiation or early growth of each organ [16]. If that were the case, *CWPO-C* would be expected to express strongly in newly generating axillary branches. The presence of the shoot apex inhibits axillary bud outgrowth in the phenomenon called apical dominance. Decapitation of the shoot tip releases the axillary buds from growth inhibition. As expected, in transgenic poplar bearing *Pcwpo-c*::*GUS*, when the tip of the main stem was cut, staining for GUS activity beneath the stem tip disappeared, and strong staining was observed in the newly developed axillary branches (Fig. 4a). In other experiments, using callus in which multiple adventitious buds were induced, similarly, strong GUS staining was observed in the adventitious buds derived from the callus (Fig. 4b). These observations strongly support the hypothesis that CWPO-C participates in plant growth and development, and specifically organogenesis at the shoot apex and axillary buds.

CWPO-C overexpression modifies growth rates

To assess the functional role of CWPO-C during poplar growth and development, we generated three independent CWPO-C overexpression (OE) lines and two independent RNAi lines. Six-week-old plants were analyzed for gene expression by RT-qPCR (Fig. 5a, b) and protein expression by western blot using an anti-CWPO-C antibody (Fig. 5c, d). Compared with WT, the expression of *CWPO-C* transcripts were quantified as 17-, 19- and 12-fold higher in OE1, OE2 and OE4, respectively (Fig. 5a). The two RNAi lines, RNAi1 and RNAi2, showed approximately 85% and 99% lower *CWPO-C* expression, respectively, compared with WT (Fig. 5b). Expressed CWPO-C protein were clearly higher in all OE lines (Fig. 5c). CWPO-C protein was not detectable in the RNAi lines, nor in WT (Fig. 5c, d). Considering

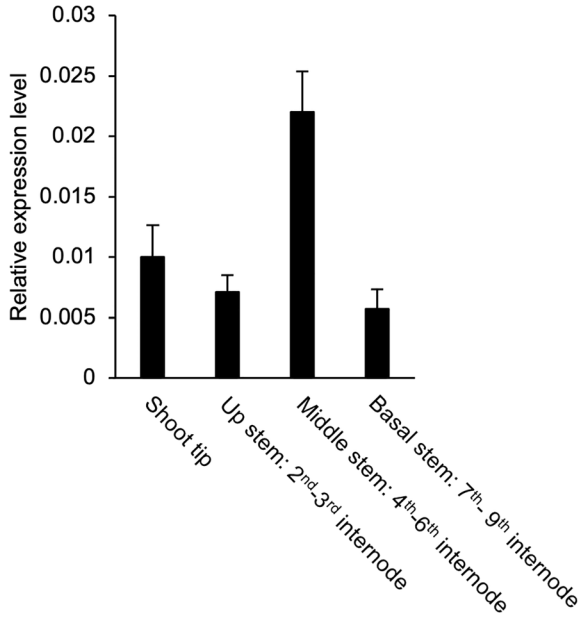

Fig. 2 Relative expression of *CWPO-C* gene in different parts of the stem in 6-week-old WT poplar. Analyses were conducted with three biological replicates (mean ± standard deviation). Data are presented as relative transcript abundance normalized to *UBQ* expression

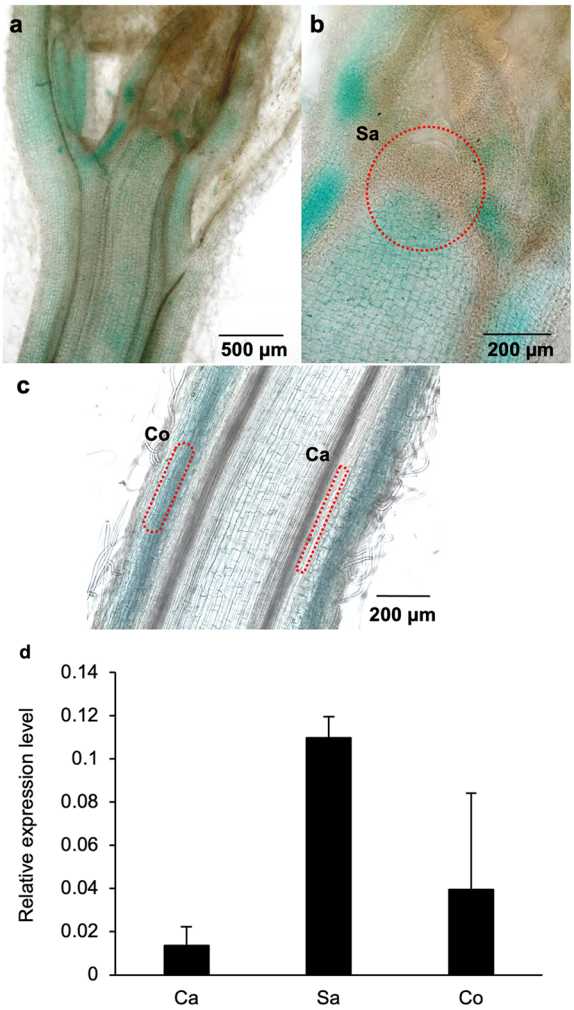

Fig. 3 Localization of *CWPO-C* transcripts**. a**–**c** Localization of GUS activity in longitudinal sections**. a, b** Stem tip. **c** Middle stem. **d** Gene expression of *CWPO-C* by RT-qPCR combined with laser micro-dissection. *Ca* cambium tissues, *Sa* shoot apex, *Co* collenchyma. Data are presented as relative transcript abundance normalized to *UBQ* expression and mean with standard deviation of triplicate analyses

both transcript and protein analyses, CWPO-C was evidently up-regulated in the three OE lines and was well-suppressed in the two RNAi lines.

The stem growth rate of *CWPO-C* overexpression lines OE1, OE2, OE4 was higher compared with WT (Additional file 1: Fig. S1b). In contrast, the growth rates of *CWPO-C* RNAi1 and RNAi2 were not significantly different from WT (Additional file 1: Fig. S1a).

The impact of CWPO-C overexpression or suppression on vascular development in the stem was observed in basal stem cross sections (Fig. 6a1–3; Additional file 1: Fig. S2a1–4). In contrast to stem elongation, stem cross-sectional area significantly increased in RNAi1 and RNAi2 (Fig. 6a2, c2; Additional file 1: Fig. S2a2, c2; Fig. 7a). This increase was mainly the result of enlargement of the cortical area (Fig. 6a, b, c, d; Additional file 1: Fig. S2a–d), and consequently the proportion of xylem in the cross section decreased (Fig. 7b). The enhancement of the cortical area in the stem seems to be a positive effect of the plant in response to the decreased proportion of xylem in the cross section (Figs. 6, 7). The decrease of xylem area is a negative effect of the CWPO-C suppression in RNAi lines. The mechanism of xylem area affected by the lower presence of CWPO-C is unknown. These results suggest that CWPO-C promoted vertical growth and differentiation of xylem, while not affecting horizontal growth.

Alteration of lignin content and composition

As shown in Fig. 1d1, 2, CWPO-C was expressed in xylem, and the protein has been shown to produce high molecular weight lignin in vitro [12]. In addition, knock-out of *CWPO-C* ortholog peroxidases, *AtPrx2*, *AtPrx25* and *AtPrx71* affected the lignin content and chemical structures in Arabidopsis [29]. Therefore, we investigated whether overexpression or suppression of *CWPO-C* in poplar might affect lignin content and composition. Transgenic lines OE1 and RNAi1 at 6 weeks were subjected to lignin analyses. Table 1 shows the lignin content determined by the acetyl bromide method and the arylglycerol-β-aryl (β-*O*-4) ether

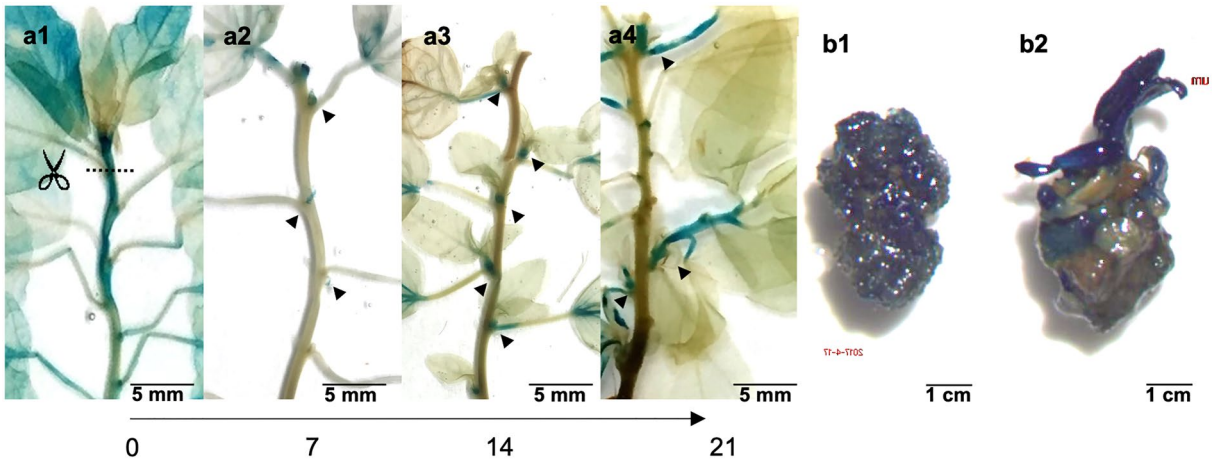

Fig. 4 *Pcwpo-c*::*GUS* expression during axillary bud outgrowth and adventitious bud induction. **a1**–**a4** Axillary bud outgrowth induction. **a1** Before stem tip decapitation (dotted line indicates decapitation position). **a2**–**a4** Sequence of axillary bud outgrowth (7, 14 and 21 days after decapitation, respectively). Black arrows indicate newly generated buds in the stem. **b1** Callus. **b2** Adventitious bud outgrowth on callus

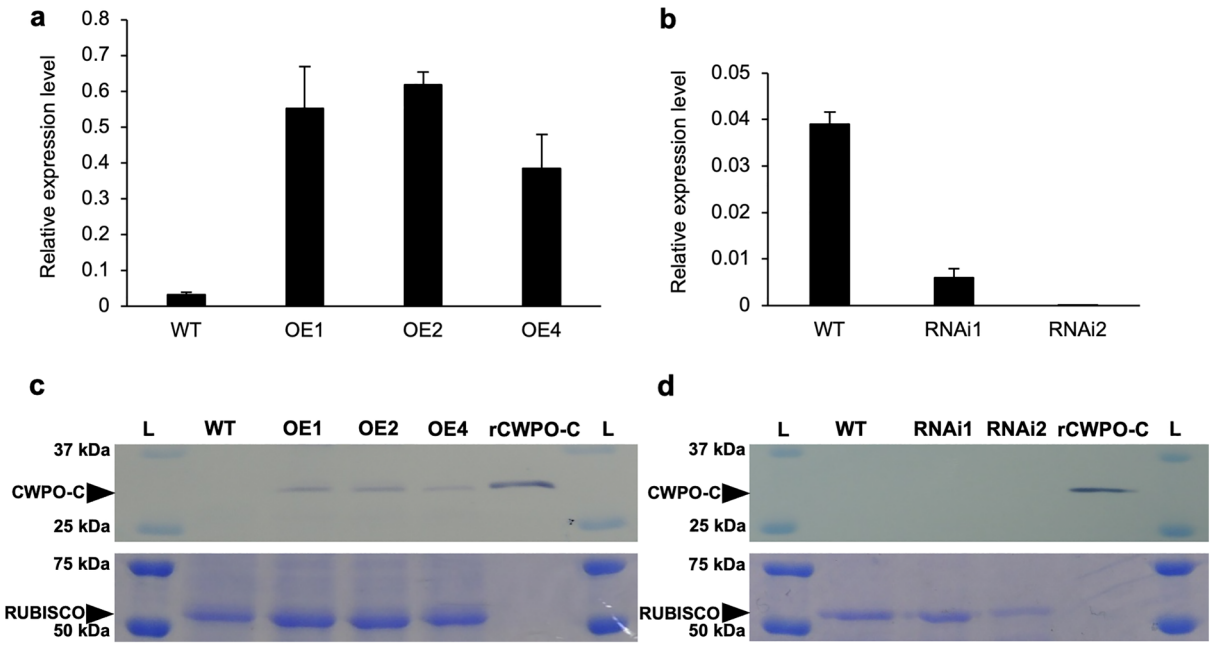

Fig. 5 Expression of *CWPO-C* and CWPO-C protein in transgenic poplar lines. **a**, **b** *CWPO-C* expression levels in 6-week-old overexpression (OE) and suppression (RNAi) transgenic poplar lines. **a** *CWPO-C* expression in WT and three OE lines. **b** *CWPO-C* expression in WT and two RNAi lines. Relative expression levels (mean ± standard deviation) measured by RT-qPCR were calculated from three biological replicates. Data are presented as relative transcript abundance normalized to *UBQ* expression. **c**, **d** Western blot analysis of CWPO-C protein in transgenic lines using an anti-CWPO-C antibody. **c** WT and three OE lines. **d** WT and two RNAi lines. Upper panels: recombinant CWPO-C protein as a standard marker (rCWPO-C, arrow). Lower panels: proteins stained with Coomassie brilliant blue; arrow indicates Rubisco. L: molecular weight markers

lignin composition, as determined by DFRC method. Lignin content in RNAi1 was significantly lower (45% decrease) than in the WT, while OE1 showed no difference from the WT (Table 1). A notable difference was found for the β-*O*-4 linkage in the lignin of RNAi1, in that the free guaiacyl monomer, coniferyl alcohol, was significantly higher than in WT (Table 1). Changes in lignin in RNAi1 were also observed using Wiesner staining of stem cross sections. The fuchsia-color staining, related to lignified cell walls, seen in the

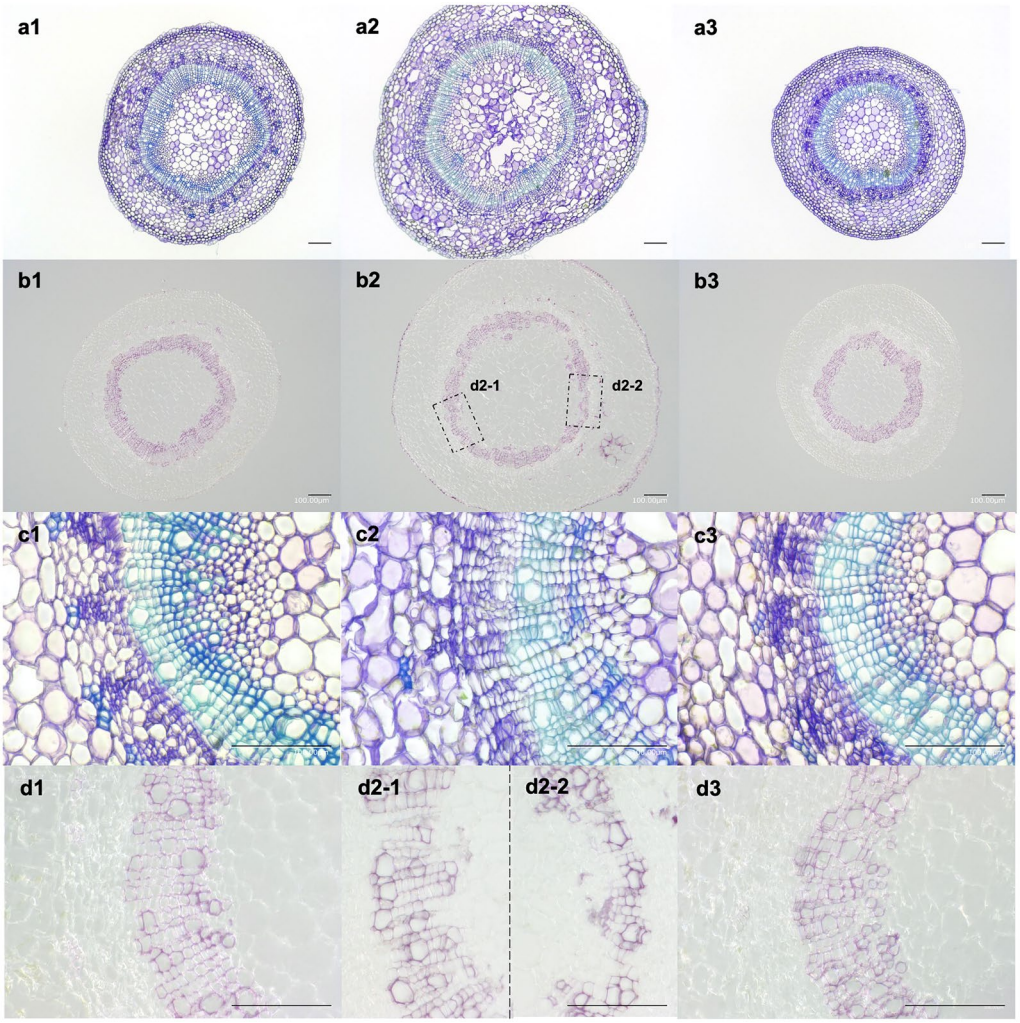

Fig. 6 Cross sections of basal stem of CWPO-C transgenic poplar lines. **a**, **c** Toluidine blue staining. **b**, **d** Wiesner staining. **a1**, **b1**, **c1**, **d1** WT. **a2**, **b2**, **c2**, **d2** RNAi suppression line RNAi1. **a3**, **b3**, **c3**, **d3** Overexpression line OE1. Sections (20 µm thick) were prepared from the basal stem of 6-week-old plants. Bar 100 µm

stem cross section was much reduced compared to the WT, and the distribution of lignified cells in the xylem was less-uniform (Fig. 6d2–1, d2–2). These chemical analyses and microscopic observations indicated that suppression of CWPO-C resulted in decreased lignin content and lower syringyl/guaiacyl (S/G) ratio in poplar.

Evaluation of relevance to auxin by gravitropism

Previously, we showed that overexpression of CWPO-C in Arabidopsis affected the phenotype strongly in way related to auxin [16]. From the results in the current study, it was clear that CWPO-C plays a role in organ development or differentiation during early growth of poplar, and it seemed possible that CWPO-C contributes to the catabolism of auxin. When a plant part is moved from a vertical to horizontal position, gravitropism occurs because of the altered distribution of auxin in the upper and lower part. In this study, we compared the time required to reach a 90° stem curvature after being placed horizontally. Transgenic OE1 plants bent more quickly than the WT, taking about half the time required by WT plants, at 8.2 h and 16.4 h, respectively (Fig. 8). Two other OE lines also showed shorter bending times than the WT. This result suggested the possibility that CWPO-C overexpression modulated the gravitropic response of the transgenic OE plants by affecting auxin accumulation. The difference in bending time between RNAi suppression lines and the WT was rather smaller but still significant (Fig. 8).

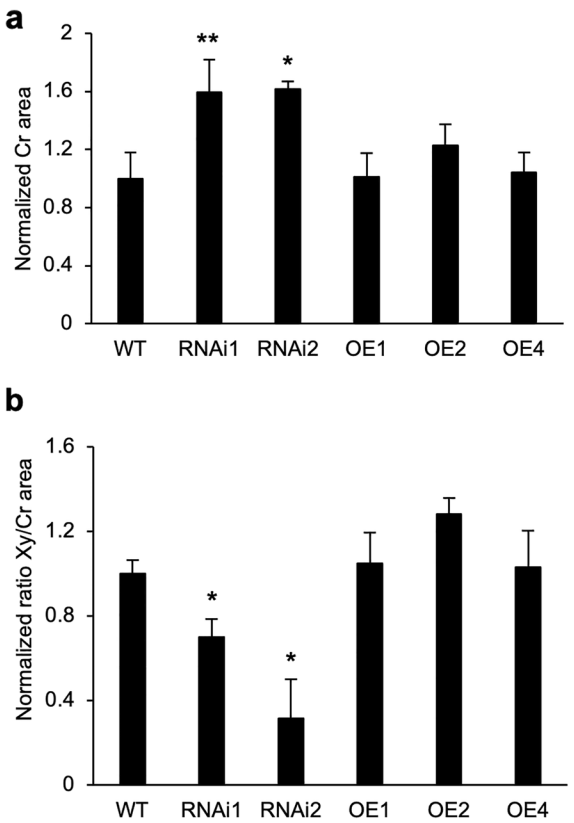

Fig. 7 Effect of CWPO-C expression on stem and xylem formation in transgenic poplar. **a** Cross-sectional (Cr) area of whole basal stem. **b** Ratio of xylem/whole cross-sectional (Xy/Cr) area. Data are presented relative to the WT, which was set to 1. Mean ± standard deviation of four biological replicates. *: significant difference ($p < 0.05$), **: significant difference ($p < 0.01$) compared with WT (Student's *t* test). OE1, OE2 and OE4: CWPO-C OE line 1, 2 and 4. RNAi1 and RNAi2: CWPO-C RNAi line 1 and 2

Table 1 Lignin content and monomer composition in WT and CWPO-C transgenic poplar

	Lignin (%)	µmol S/g lignin	µmol G/g lignin	S/G	µmol (S + G)/g lignin
WT	9.2 ± 0.8	61 ± 20	428 ± 40	0,14 ± 0,03	489 ± 60
RNAi1	5.1 ± 0.6[b]	51 ± 14	717 ± 81[b]	0,07 ± 0,01[a]	768 ± 93[b]
OE1	8.8 ± 0.9	45 ± 14	381 ± 74	0,12 ± 0,03	426 ± 84

Lignin content and monomer composition were measured by derivatization followed by reductive cleavage (DFRC). Lignin contents are presented as percentage of cell wall dry weight. Data presented as mean ± standard deviation from four independent biological replicates. Letters indicate significant differences between transgenic line and WT control

G, S Guaiacyl and syringyl monomers, respectively

[a] $p < 0.05$

[b] $p < 0.01$, Student's *t* test

Another notable phenotype related to auxin modification was found in the leaves: transgenic line OE1 showed more rounded leaf shape with less pronounced saw-tooth edges, while line RNAi1 had larger leaves with light green color, compared to the WT (Additional file 1: Fig. S3). Because the hydathodes, at the leaf edge, where notches develop, coincided with the expression site of CWPO-C (Additional file 1: Fig. S4), we hypothesize that CWPO-C might function in an inhibitory manner on saw-tooth leaf formation in OE lines, resulting in the more rounded leaves.

Discussion

Previously, CWPO-C has been considered to be specifically involved in the lignification process of cell walls, since our previous research indicated that CWPO-C has a unique oxidative activity toward monolignols and lignin polymer [12, 13]. However, our recent findings showed that *CWPO-C* was expressed in immature tissues, such apical meristem, young upper stems, developing xylem and young leaves in *Arabidopsis thaliana* transformed with *Pcwpo-c*::*GUS* [16]. In the current study, our results using poplar with the same *Pcwpo-c*::*GUS* construct indicated similar characteristic expression sites of *CWPO-C*, namely, the upper stem, developing stem xylem and cortex, petiole, root and young leaves, including trichomes and stomata (Fig. 1a, b1, d1; Additional file 1: Fig. S4b, c). These locations were substantially consistent with our previous report using heterologous promoter assays in Arabidopsis (summarized in Table 2). Therefore, it can be concluded that *CWPO-C* is expressed mainly in young tissues after differentiation, rather than organs, such as flowers and seeds, and is involved in the development or differentiation of organs and early growth. Interestingly, decapitation of poplar transformed with *Pcwpo-c*::*GUS* led to *CWPO-C* expression in the axillary meristems and in the newly generated branches. This result clearly shows that CWPO-C is involved in plant growth and development.

Several previous studies analyzed the functions of peroxidases by a reverse genetic approach in which targeted gene expression was suppressed or enhanced. In tobacco, tobacco transformants with suppressed anionic peroxidase (TOBPXDLF) showed an enhanced growth rate [30]. Overexpression of HRP, encoded by *prxC1a*, in hybrid poplar resulted in higher growth rates [18]. These findings suggest that peroxidases have multiple roles during growth and development. In our current results, CWPO-C OE poplar lines (OE1, OE2, OE4) showed higher growth rates than the WT (Additional file 1: Fig. S1b), yet there was no altered growth rate in CWPO-C

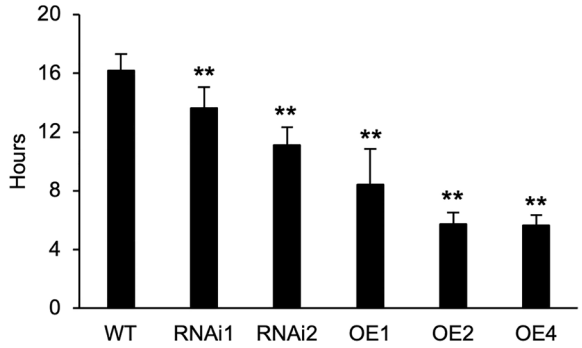

Fig. 8 Bending time of 6-week-old CWPO-C transgenics and WT poplar. Bending time refers to the time (h) required for the stem to return to standing at 90° from being placed horizontally. Mean ± standard deviation of four biological replicates. **: significant difference ($p < 0.01$) compared with WT (Student's *t* test). OE1, OE2 and OE4: CWPO-C OE line 1, 2 and 4. RNAi1 and RNAi2: CWPO-C RNAi line 1 and 2

RNAi suppression lines. Auxin is known to activate cell elongation by increasing cell wall extensibility [31]. Interaction has been reported between auxin and peroxidase, and can be divided broadly into two types: induction by auxin of peroxidases responsible for lignification, and auxin catabolism by peroxidases. For example, the overexpression of *CpPrx01* from *Cucurbita pepo* in Arabidopsis led to longer roots and hypocotyls, at the same time reducing levels of the auxin indole-3-acetic acid (IAA) [5]. PxB2 from *Vitis vinifera* was found to have oxidative activity toward IAA, suggesting it played a role in controlling the amount of IAA in developing roots [32]. There have been no conclusive report on the cellular level localization, where peroxidases interact with auxin in our knowledge. It is known that IAA is transported between cells through the apoplast, and IAA oxidase activity (catabolism) mainly occurs in the apoplast [33, 34]. Since CWPO-C was reported to be ionically bound cell wall peroxidase [35], thus localized in the apoplast [36], we could predict that IAA catabolism by CWPO-C may occur in the apoplast. A gravitropism test is a traditional and simple method to observe alterations of auxin concentration. Here, the poplar CWPO-C OE lines, showed shorter recovery times for the stem to return to the vertical position (Fig. 8), which suggested that auxin amounts might be increased by the overexpression of *CWPO-C*. However, observations in Arabidopsis with overexpressing *CWPO-C* showed differences compared with the poplar OE lines [16]: the CWPO-C OE Arabidopsis showed significantly longer recovery time (negative gravitropism) than the wild type. The negative gravitropism was explained by a marked decrease of auxin content in CWPO-C OE Arabidopsis [16]. In addition, in Arabidopsis, CWPO-C OE caused severe suppression of stem elongation, whereas in poplar CWPO-C OE caused slightly enhanced stem elongation. One possible explanation for this apparent discrepancy is that poplar has a higher capability for maintenance of homeostasis against changes in auxin conditions. Another explanation is that such different phenotypes may be the result of different physiological responses between poplar and Arabidopsis, depending on the auxin concentration, as hypothesized in the schematic diagram (Additional file 1: Fig. S5). In our previous study, the stem tip of Arabidopsis possessed approx. 2 ng/mg FW of IAA [16]. Teichmann et al. [37] showed that 4-month-old stem tips in poplar contained approx. 0.08 ng/mg FW of IAA. Sitbon et al. [38] showed

Table 2 Expression sites of *CWPO-C* in WT poplar and Arabidopsis

Organ/Plant	*P. alba*	3-Day-old *A. thaliana*	3-Week-old *A. thaliana*	5-Week-old *A. thaliana*
Stem meristem	Shoot apex	Shoot apex	Shoot apex	Shoot apex
Upper stem	Xylem	n.a.	n.t.	Xylem
Middle/lower stem	Xylem, cortex, petiole base	n.a.	n.t.	Cortex around cauline leaf base
Petiole	Entirely	n.a.	n.d.	Entirely
Root	Entirely except the tip	Entirely except the tip	Entirely except the tip	n.t.
Flower	n.a.	n.a.	n.t.	Flower bud
Fruit	n.a.	n.a.	n.a.	Inmature siliques and seeds
Upper leaves	Entirely	n.a.	Entirely, hydathodes	n.t.
Middle/lower leaves	Tip, hydathodes, trichome, stomata	n.a.	Tip, hydathodes	Tip, hydathodes
Axillary bud	Entirely	n.a.	n.t.	Entirely
Cotyledon	n.a.	Tip, trichome, stomata	n.a.	n.a.
Hypocotyl	n.a.	Around cotyledon and root base	n.a.	n.a.

Arabidopsis data in Yoshikay-Benitez et al. [16]

n.t. not tested, *n.a.* not applicable, *n.d.* not detected

that tobacco shoot apex contained approx. 0.05 ng/mg FW of IAA. These reports suggested that the response and optimum concentrations of IAA are differed widely, depending on the plant species. It is also known that the reaction of plants to auxin differs, depending not only on the plant species, but also on the organ [39–41]. In our previous report, recombinant CWPO-C protein broke down IAA in vitro, and IAA concentration in CWPO-C OE Arabidopsis was considerably reduced. Thus, in Arabidopsis we concluded that overexpressed CWPO-C decreased endogenous IAA concentration. In our study, the observed effects of the CWPO-C OE on growth rate and bending time in poplar were directly opposite to those in Arabidopsis. A possible explanation for the different phenotypes is shown in Additional file 1: Fig. S5, where the endogenous IAA concentration decreased toward the optimum in poplar, whereas it decreased away from the optimum in Arabidopsis. Concerning the bending time, the mechanisms affecting bending time seems complicated. It seems difficult to explain relation of bending time and IAA concentration. The observed faster bending time of the CWPO-C OE poplar was opposite to CWPO-C OE Arabidopsis which showed the slower bending time. In addition, CWPO-C RNAi poplar showed a slightly faster or similar bending time than WT. In the case of poplar, it seems difficult to explain the changes of bending time by only IAA, and there are some other predominant factors for controlling the bending speed in poplar.

We considered the function of CWPO-C in lignification, because *CWPO-C* was expressed in the developing xylem during its progression to lignification, and *CWPO-C* suppression might affect the lignin content and S/G composition. Previously, three *CWPO-C* orthologs (*AtPrx2*, *AtPrx25*, and *AtPrx71*) were knocked out in Arabidopsis, and decreased lignin content was observed [29, 42]. Suppression of *NtPrx60* and *PrxA3a* genes in tobacco and aspen, respectively, also reduced the lignin content [43, 44]. Knockout of orthologous genes (*AtPrx4*, *AtPrx52* and *AtPrx72*) of *Zinnia elegans* peroxidase, *ZePrx*, showed reduced lignin content and altered lignin composition [45–47]. In our current study, lignin content was reduced by 45% in the CWPO-C-suppressed poplar, and the S/G ratio of lignin in RNAi1 (determined by DFRC analysis) was half that of WT (Table 1). A noticeable increase in the content of the guaiacyl monomer, coniferyl alcohol, resulted in the decreased S/G ratio. The increase of guaiacyl monomer might be explained by an increase in β-*O*-4 linkage in guaiacyl lignin by the suppression of *CWPO-C*. It seems unlikely that suppression of a single peroxidase, an enzyme catalyzing the polymerization of monolignol, directly enhanced the biosynthesis of coniferyl alcohol. An alternative explanation might be that *CWPO-C* suppression changed the allocation of S/G monolignol monomers at branch points in the biosynthetic pathway. The suppression of peroxidase activity might slow down the monolignol polymerization rate in the cell wall, so that the proportion of β-*O*-4 linkages increased in lignin through slower end-polymerization. This effect would be more prominent in guaiacyl lignin, because guaiacyl lignin was predominant in the young poplar plants used in this study. Previously, we observed a similar increase in the yield of DFRC products in knockout mutants of *AtPrx2*, *AtPrx25*, and *AtPrx71* [29, 42]. These results confirmed that CWPO-C and its Arabidopsis orthologs play a substantive role in lignin polymerization in the cell wall.

Abbreviations

ABSL	Acetyl bromide-soluble lignin
CWPO-C	Cationic cell-wall-bound peroxidase
DFRC	Derivatization followed by reductive cleavage
GC–FID	Gas chromatography–flame ionization detector
GUS	β-Glucuronidase
LMD	Laser micro-dissection
OE	Overexpression
RNAi	RNA interference
RT-qPCR	Real-time quantitative PCR
S/G ratio	Syringyl/guaiacyl ratio
TDZ	Thidiazuron

Supplementary Information

The online version contains supplementary material available at https://doi.org/10.1186/s10086-023-02086-1.

Additional file 1: Fig. S1 Effect of CWPO-C expression on stem growth in CWPO-C transgenic lines. **a** RNAi suppression lines 1 and 2. **b** Overexpression lines OE1, 2 and 4. Different letters represent significant differences. Lower-case letter: significant difference ($p < 0.05$), upper-case letter: significant difference ($p < 0.01$) compared with WT (Student's *t* test). Four biological replicates were analyzed, and data are presented as the mean ± standard deviation. **Fig. S2** Cross sections of basal stem of CWPO-C transgenic poplar lines. **a, c** Toluidine blue staining. **b, d** Wiesner staining. **a1, b1, c1, d1** WT. **a2, b2, c2, d2** RNAi suppression line RNAi2. **a3, b3, c3, d3** Overexpression line OE2. **a4, b4, c4, d4** Overexpression line OE4. Sections (20 µm thick) were prepared from the basal stem of 6-week-old plants. Bar 100 µm. **Fig. S3** Leaf phenotype in CWPO-C transgenic poplar lines. **a** Leaf color and border shape. Left to right: WT, OE1 and RNAi1. **b** Leaves in 6-week-old poplar. Left to right: younger to older leaves. Upper row: WT; middle row: OE1; lower row: RNAi1. **Fig. S4** *GUS* expression driven by *CWPO-C* promoter in poplar leaf. **a** Leaf. **a1** Hydathode. **b** Trichome (black arrows: base of trichome). **c** Stomata (black arrow: stoma). **Fig. S5** Schematic representation of possible responses to altered *CWPO-C* expression in Arabidopsis and poplar. Stem elongation is promoted or inhibited over a range of auxin concentration, depending on the plant species and the effect of *CWPO-C* expression on auxin catabolism. In both poplar and Arabidopsis, overexpressed CWPO-C decreases IAA concentration via catabolism. In Arabidopsis, decreased IAA concentration leads to reduced elongation growth. In poplar, by contrast, overexpressed CWPO-C again decreases IAA concentration, but leads to enhanced elongation. The difference in apparent effects is presumed to result from different responses toward IAA concentration in the two plant species.

Acknowledgements
We thank Edanz (https://jp.edanz.com/ac) for editing a draft of this manuscript.

Author contributions
YT was the principal investigator of this project and JS was the sub-principal investigator. DAY-B and JS designed the experiments. DAY-B, KO, KB and KF performed the experiments and analyzed the data. DAY-B and JS wrote the manuscript. YT and JS revised the manuscript. All authors read and approved the final manuscript.

Funding
This work was supported by JSPS Grants-in-Aid for Scientific Research (KAKENHI) (Grant Numbers JP17H03846 and 20H03046) and a JSPS Grant-in-Aid for Exploratory Research (Grant Number 18K19234).

Availability of data and materials
Data sharing is not applicable to this article as no data sets were generated or analyzed during the current study.

Declarations

Competing interests
The authors declare that they have no competing interests.

Received: 30 November 2022 Accepted: 10 February 2023
Published online: 28 February 2023

References

1. Ren LL, Liu YJ, Liu HJ, Qian TT, Qi LW, Wang XR, Zeng QY (2014) Subcellular relocalization and positive selection play key roles in the retention of duplicate genes of *Populus* class III peroxidase family. Plant Cell 26:2404–2419. https://doi.org/10.1105/tpc.114.124750
2. Shigeto J, Tsutsumi Y (2015) Diverse functions and reactions of class III peroxidases. New Phytol 209(4):1395–1402. https://doi.org/10.1111/nph.13738
3. Hoffmann N, Benske A, Betz H, Schuetz M, Samuels AL (2020) Laccases and peroxidases co-localize in lignified secondary cell walls throughout stem development. Plant Physiol 184(2):806–822. https://doi.org/10.1104/pp.20.00473
4. Almagro L, Gómez Ros LV, Belchi-Navarro S, Bru R, Ros Barceló A, Pedreño MA (2009) Class III peroxidases in plant defence reactions. J Exp Bot 60(2):377–390. https://doi.org/10.1093/jxb/ern277
5. Cosio C, Vuillemin L, De Meyer M, Kevers C, Penel C, Dunand C (2009) An anionic class III peroxidase from zucchini may regulate hypocotyl elongation through its auxin oxidase activity. Planta 229:823–836. https://doi.org/10.1007/s00425-008-0876-0
6. Müller K, Linkies A, Vreeburg RA, Fry SC, Krieger-Liszkay A, Leubner-Metzger G (2009) *In vivo* cell wall loosening by hydroxyl radicals during cress seed germination and elongation growth. Plant Physiol 150:1855–1865. https://doi.org/10.1104/pp.109.139204
7. Kunieda T, Shimada T, Kondo M, Nishimura M, Nishitani K, Hara-Nishimura I (2013) Spatiotemporal secretion of PEROXIDASE36 is required for seed coat mucilage extrusion in *Arabidopsis*. Plant Cell 25:1355–1367. https://doi.org/10.1105/tpc.113.110072
8. Jemmat AM, Ranocha P, Le Ru A, Neel M, Jauneau A, Raggi S, Ferrari S, Burlat V, Dunand C (2020) Coordination of five class III peroxidase-encoding genes for early germination events of *Arabidopsis thaliana*. Plant Sci 298:110565. https://doi.org/10.1016/j.plantsci.2020.110565
9. Renard J, Martínez-Almonacid I, Sonntag A, Molina I, Moya-Cuevas J, Bissoli G, Muñoz-Bertomeu J, Faus I, Niñoles R, Shigeto J, Tsutsumi Y, Gadea J, Serrano R, Bueso E (2020) *PRX2* and *PRX25*, peroxidases regulated by COG1, are involved in seed longevity in *Arabidopsis*. Plant Cell Environ 43:315–326. https://doi.org/10.1111/pce.13656
10. Boerjan W, Ralph J, Baucher M (2003) Lignin biosynthesis. Annu Rev Plant Biol 54:519–546. https://doi.org/10.1146/annurev.arplant.54.031902.134938
11. Sarkanen KV, Ludwig CH (1971) Lignins, occurrence, formation structure and reactions. John Wiley & Sons Inc, New York
12. Aoyama W, Sasaki S, Matsumura S, Hirai H, Tsutsumi Y, Nishida T (2002) Sinapyl alcohol-specific peroxidase isoenzyme catalyzes the formation of the dehydrogenative polymer from sinapyl alcohol. J Wood Sci 48:497–504. https://doi.org/10.1007/BF00766646
13. Sasaki S, Nishida T, Tsutsumi Y, Kondo R (2004) Lignin dehydrogenative polymerization mechanism: a poplar cell wall peroxidase directly oxidizes polymer lignin and produces *in vitro* dehydrogenative polymer rich in beta-*O*-4 linkage. FEBS Lett 562:197–201. https://doi.org/10.1016/S0014-5793(04)00224-8
14. Sasaki S, Nonaka D, Wariishi H, Tsutsumi Y, Kondo R (2008) Role of Tyr residues on the protein surface of cationic cell-wall-peroxidase (CWPO-C) from poplar: potential oxidation sites for oxidative polymerization of lignin. Phytochemistry 69(2):348–355. https://doi.org/10.1016/j.phytochem.2007.08.020
15. Shigeto J, Itoh Y, Tsutsumi Y, Kondo R (2012) Identification of Tyr74 and Tyr177 as substrate oxidation sites in cationic cell wall-bound peroxidase from *Populus alba* L. FEBS J 279:348–357. https://doi.org/10.1111/j.1742-4658.2011.08429.x
16. Yoshikay-Benitez DA, Yokoyama Y, Ohira K, Fujita K, Tomie A, Kijidani Y, Shigeto J, Tsutsumi Y (2022) *Populus alba* cationic cell-wall-bound peroxidase (CWPO-C) regulates the plant growth and affects auxin concentration in *Arabidopsis thaliana*. Physiol Mol Biol Plants 28:1671–1680. https://doi.org/10.1007/s12298-022-01241-0
17. Kawaoka A, Kawamoto T, Moriki H, Murakami A, Murakami K, Yoshida K, Sekine M, Takano M, Shinmyo A (1994) Growth-stimulation of tobacco plant introduced the horseradish peroxidase gene *prxC1a*. J Ferment Bioeng 78(1):49–53. https://doi.org/10.1016/0922-338X(94)90177-5
18. Kawaoka A, Matsunaga E, Endo S, Kondo S, Yoshida K, Shinmyo A, Ebinuma H (2003) Ectopic expression of a horseradish peroxidase enhances growth rate and increases oxidative stress resistance in hybrid aspen. Plant Physiol 132(3):1177–1185. https://doi.org/10.1104/pp.102.019794
19. Takata N, Eriksson ME (2012) A simple and efficient transient transformation for hybrid aspen *(Populus tremula* × *P tremuloides)*. Plant Methods 8:30. https://doi.org/10.1186/1746-4811-8-30
20. Song C, Lu L, Guo Y, Xu H, Li R (2019) Efficient *Agrobacterium*-mediated transformation of the commercial hybrid poplar *Populus Alba* × *Populus glandulosa* uyeki. Int J Mol Sci 20:2594. https://doi.org/10.3390/ijms20102594
21. Nanasato Y, Kido M, Kato A, Ueda T, Suharsono S, Widyastuti U, Tsujimoto H, Akashi K (2015) Efficient genetic transformation of *Jatropha curcas* L. by means of vacuum infiltration combined with filter-paper wicks. In Vitro Cell Dev Biol -Plant 51:399–406. https://doi.org/10.1007/s11627-015-9703-z
22. Abbott E, Hall D, Hamberger B, Bohlmann J (2010) Laser microdissection of conifer stem tissues: Isolation and analysis of high quality RNA, terpene synthase enzyme activity and terpenoid metabolites from resin ducts and cambial zone tissue of white spruce (*Picea glauca*). BMC Plant Biol 10:106. https://doi.org/10.1186/1471-2229-10-106
23. Takeuchi M, Watanabe A, Tamura M, Tsutsumi Y (2018) The gene expression analysis of *Arabidopsis thaliana* ABC transporters by real-time PCR for screening monolignol-transporter candidates. J Wood Sci 64:477–484. https://doi.org/10.1007/s10086-018-1733-9
24. Vitha S, Beneš K, Michalová M, Ondřej M (1993) Quantitative β-glucuronidase assay in transgenic plants. Biol Plant 35:151–155. https://doi.org/10.1007/BF02921141
25. Barnes WJ, Anderson CT (2017) Acetyl bromide soluble lignin (ABSL) assay for total lignin quantification from plant biomass. Bio Protoc 7(5):e2149. https://doi.org/10.2176/BioProtoc.2149
26. Lu F, Ralph J (1997) Derivatization followed by reductive cleavage (DFRC method), a new method for lignin analysis: protocol for analysis of DFRC monomers. J Agric Food Chem 45(7):2590–2592. https://doi.org/10.1021/jf970258h
27. Pradhan Mitra P, Loqué D (2014) Histochemical staining of *Arabidopsis thaliana* secondary cell wall elements. J Vis Exp 87:51381. https://doi.org/10.3791/51381
28. Euring D, Löfke C, Teichmann T, Polle A (2012) Nitrogen fertilization has differential effects on N allocation and lignin in two *Populus* species with contrasting ecology. Trees 26:1933–1942. https://doi.org/10.1007/s00468-012-0761-0

29. Shigeto J, Kiyonaga Y, Fujita K, Kondo R, Tsutsumi Y (2013) Putative cationic cell-wall-bound peroxidase homologues in *Arabidopsis*, AtPrx2, AtPrx25, and AtPrx71, are involved in lignification. J Agric Food Chem 61:3781–3788. https://doi.org/10.1021/jf400426g
30. Lagrimini LM, Gingas V, Finger F, Rothstein S, Liu T (1997) Characterization of antisense transformed plants deficient in the tobacco anionic peroxidase. Plant Physiol 114(4):1187–1196. https://doi.org/10.1104/pp.114.4.1187
31. Hoson T (1993) Regulation of polysaccharide breakdown during auxin-induced cell wall loosening. J Plant Res 106:369–381. https://doi.org/10.1007/BF02345982
32. Vatulescu AD, Fortunato AS, Sá MC, Amâncio S, Ricardo CP, Jackson PA (2004) Cloning and characterisation of a basic IAA oxidase associated with root induction in *Vitis vinifera*. Plant Physiol Biochem 42(7–8):609–615. https://doi.org/10.1016/j.plaphy.2004.06.009
33. Waldrum JD, Davies E (1981) Subcellular localization of IAA oxidase in peas. Plant Physiol 68(6):1303–1307. https://doi.org/10.1104/pp.68.6.1303
34. García-Florenciano E, Calderón AA, R. Muñoz R, Ros Barceló A, (1992) The decarboxylative pathway of Indole-3-acetic acid catabolism is not functional in grapevine protoplasts. J Exp Bot 43(5):715–721. https://doi.org/10.1093/jxb/43.5.715
35. Tsutsumi Y, Matsui K, Sakai K (1998) Substrate-specific peroxidases in woody angiosperms and gymnosperms participate in regulating the dehydrogenative polymerization of syringyl and guaiacyl type lignins. Holzforsch 52(3):275–281. https://doi.org/10.1515/hfsg.1998.52.3.275
36. Sasaki S, Baba K, Nishida T, Tsutsumi Y, Kondo R (2006) The cationic cell-wall-peroxidase having oxidation ability for polymeric substrate participates in the late stage of lignification of *Populus alba* L. Plant Mol Biol 62(6):797–807. https://doi.org/10.1007/s11103-006-9057-3
37. Teichmann T, Bolu-Arianto WH, Olbrich A, Langenfeld-Heyser R, Göbel C, Grzeganek P, Feussner I, Hänsch R, Polle A (2008) GH3::GUS reflects cell-specific developmental patterns and stress-induced changes in wood anatomy in the poplar stem. Tree Physiol 28(9):1305–1315. https://doi.org/10.1093/treephys/28.9.1305
38. Sitbon F, Hennion S, Sundberg B, Little CH, Olsson O, Sandberg G (1992) Transgenic tobacco plants coexpressing the agrobacterium tumefaciens *iaaM* and *iaaH* genes display altered growth and indoleacetic acid metabolism. Plant Physiol 99(3):1062–1069. https://doi.org/10.1104/pp.99.3.1062
39. Thimann KV (1969) The auxins. In: Wilkins MB (ed) The physiology of plant growth and development. McGraw-Hill Publishing Company Limited, London, pp 1–45
40. Leopold AC (1955) Auxins and plant growth. University of California Press, Berkeley and Los Angeles
41. Gaspar T, Kevers C, Faivre-Rampant O, Crèvecoeur M, Penel CL, Greppin H, Dommes J (2003) Changing concepts in plant hormone action. In Vitro Cell Dev Biol Plant 39:85–106. https://doi.org/10.1079/IVP2002393
42. Shigeto J, Itoh Y, Hirao S, Ohira K, Fujita K, Tsutsumi Y (2015) Simultaneously disrupting *AtPrx2*, *AtPrx25* and *AtPrx71* alters lignin content and structure in *Arabidopsis* stem. J Integr Plant Biol 57:349–356. https://doi.org/10.1111/jipb.12334
43. Blee KA, Choi JW, O'Connell AP, Schuch W, Lewis NG, Bolwell GP (2003) A lignin-specific peroxidase in tobacco whose antisense suppression leads to vascular tissue modification. Phytochemistry 64(1):163–176. https://doi.org/10.1016/S0031-9422(03)00212-7
44. Li Y, Kajita S, Kawai S, Katayama Y, Morohoshi N (2003) Down-regulation of an anionic peroxidase in transgenic aspen and its effect on lignin characteristics. J Plant Res 116:175–182. https://doi.org/10.1007/s10265-003-0087-5
45. Fernández-Pérez F, Vivar T, Pomar F, Pedreño MA, Novo-Uzal E (2015) Peroxidase 4 is involved in syringyl lignin formation in *Arabidopsis thaliana*. J Plant Physiol 175:86–94. https://doi.org/10.1016/j.jplph.2014.11.006
46. Fernández-Pérez F, Pomar F, Pedreño MA, Novo-Uzal E (2015) The suppression of *AtPrx52* affects fibers but not xylem lignification in *Arabidopsis* by altering the proportion of syringyl units. Physiol Plantarum 154:395–406. https://doi.org/10.1111/ppl.12310
47. Herrero J, Fernández-Pérez F, Yebra T, Novo-Uzal E, Pomar F, Pedreño MA, Cuello J, Guéra A, Esteban-Carrasco A, Zapata JM (2013) Bioinformatic and functional characterization of the basic peroxidase 72 from *Arabidopsis thaliana* involved in lignin biosynthesis. Planta 237:1599–1612. https://doi.org/10.1007/s00425-013-1865-5

Publisher's Note